

Rhizaria in the oligotrophic ocean exhibit clear temporal and vertical variability.

Alex Barth^{*1,2}, Leocadio Blanco-Berical³, Rod Johnson³ and Joshua Stone¹

1. University of South Carolina, Biological Sciences, 700 Sumter St 401, Columbia, SC 29208
2. University of Texas at Austin, Marine Science Institute, 750 Channel Drive, Port Aransas, Texas, USA
3. Arizona State University, School of Ocean Futures, Bermuda Institute of Ocean Sciences 17 Biological Station, St Georges, GE 01

Abstract

Recently studies have shown that Rhizaria, a super-group of marine protists, have a large role in pelagic ecosystems. They are unique in that they construct mineral tests out of silica, calcium carbonate, or strontium sulfate. As a consequence, Rhizaria can have large impacts on the ocean's cycling of carbon and other elements. However, less is known about Rhizaria ecology or their role in the pelagic food-web. Some taxa, like certain Radiolarians, are mixotrophic, hosting algal symbionts. While other taxa are flux-feeders or even predatory carnivores. Some prior research has suggested that Rhizaria will partition vertically in the water column, likely due to different trophic strategies. However, very few studies have investigated their populations over extended periods of time. In this study, we present data investigating Rhizaria abundance and vertical distribution from over a year of monthly cruises in the Sargasso Sea. This study represents the first quantification of Rhizaria throughout the mesopelagic zone in an oligotrophic system for an extended period of time. We use this data to investigate the hypothesis that Rhizaria taxonomic groups will partition due to trophic mode. We also investigate how their abundance varies in accordance with environmental parameters. Rhizaria abundance was quantified using an Underwater Vision Profiler (UVP5), an in-situ imaging device. Ultimately, we show that different Rhizaria taxa will have unique vertical distribution patterns. Models relating their abundance to environmental parameters have mixed results, yet particle concentration is a common predictive variable, supporting the importance of heterotrophy amongst many taxa.

2 Introduction

3 Rhizaria are an extremely diverse super-group of single-celled organisms consisting of several phyla including
4 Retaria (foraminifera and radiolaria) and Cercozoa. These organisms exist in a wide range of habitats
5 and are widely represented in plankton communities throughout the global ocean. While the taxonomy
6 of these organisms has recently undergone several reclassifications (Biard, 2022a), their presence in ocean
7 ecosystems has been long known to oceanographers. Some of the earliest records of their existence are from
8 oceanographic expeditions in the 19th century (Haekel, 1887). Rhizaria are unique members of the plankton
9 and protist community because they can reach large sizes (up to several mm in diameter) and they construct
10 intricate mineral skeletons out of either silica, strontium, or calcium carbonate (Biard, 2022a; Kimoto,
11 2015; Nakamura and Suzuki, 2015; Suzuki and Not, 2015). Despite their noticeable morphology and global
12 distribution, Rhizaria were largely understudied throughout the 20th century. The bulk of modern plankton
13 research has focused on hard-bodied crustacea which are numerically dominant and easily sampled with nets
14 and preservatives. Fragile organisms like Rhizaria were difficult to adequately study as they can be destroyed
15 through standard zooplankton sampling techniques and preserve poorly. A number of studies in the late
16 1900s did employ alternative techniques to quantify Rhizaria including diaphragm pumps (Michaels, 1988)
17 or blue-water SCUBA collections (Bijma et al., 1990; Caron et al., 1995; Caron and Be, 1984). However, the
18 bulk of Rhizaria research was constrained to sediment traps or paleontological studies of sediment (Boltovskoy
19 et al., 1993; Takahashi et al., 1983). Only recently has the advent of molecular techniques and in-situ imaging
20 tools ignited a renewed focus on Rhizaria in pelagic ecosystems (Caron, 2016).

21 The wave of new data on Rhizaria has facilitated an improved understanding of the significance in ocean
22 ecosystem functions. Firstly, taxonomists have been able to greatly refine the understanding of evolutionary
23 relationships amongst these diverse protists (Aurahs et al., 2009; Biard et al., 2015; Cavalier-Smith et al.,
24 2018; Decelle et al., 2013, 2012; rev by Biard, 2022a). DNA metabarcoding studies have revealed insights

25 into the distributional patterns (Biard et al., 2017; Blanco-Bercial et al., 2022; Decelle et al., 2013; Llopis
26 Monferrer et al., 2022; Mars Brisbin et al., 2020; Sogawa et al., 2022), ecological relationships (Decelle et
27 al., 2012; Nakamura et al., 2023), and contribution to biogeochemical fluxes (Guidi et al., 2016; Gutierrez-
28 Rodriguez et al., 2019). Transcriptomic and proteomic approaches also have been used to quantify Rhizaria
29 contribution to community metabolism (Cohen et al., 2023). Yet, despite the excellent taxonomic resolution
30 provided by molecular approaches, they do not provide a truly quantitative metric for estimating Rhizaria
31 abundance or biomass. In-situ imaging tools however, offer the ability to observe organisms in the natural
32 state and quantify their abundance (Barth and Stone, In press; Ohman, 2019). Biard et al. (2016) utilized
33 in-situ imaging at a global scale to suggest Rhizaria were substantial contributors to the ocean carbon
34 standing stock. While more recent calculations suggest lower carbon contribution (Laget et al., 2024),
35 Rhizaria nonetheless have substantial influences on biogeochemical cycling. Due to their large sizes, ability to
36 concentrate smaller particles and the unique structure of their mineral skeletons, Rhizaria have the potential
37 to massively influence ocean biogeochemical cycling. A number of studies have made large advances in
38 estimating the contribution of Rhizaria to ocean cycling of carbon (Gutierrez-Rodriguez et al., 2019; Ikenoue
39 et al., 2019; Lampitt et al., 2009; Stukel et al., 2018), silica (Biard et al., 2018; Llopis Monferrer et al., 2021),
40 and strontium (Decelle et al., 2013). Still, Rhizaria ecological roles are not well understood (Biard, 2022a).
41 This is a major challenge as it is critical to understand the ecological role of plankton to fully incorporate
42 them into biological oceanographic models.

43 The ecological role of Rhizaria in plankton communities is complicated due to the fact different taxa can
44 exhibit every different trophic modes. As zooplankton, rhizaria are predominately heterotrophic (Biard,
45 2022a), yet their feeding modes can be quite varied. Phaeodarias (family Cercozoa) are largely thought to
46 be flux-feeders, collecting and feeding on sinking particles (Nakamura and Suzuki, 2015; Stukel et al., 2019).
47 Alternatively, Retaria can be either exclusively heterotrophic or mixotrophic, utilizing photosynthetic algal

48 symbionts (Anderson, 2014; Decelle et al., 2015). Mixotrophic foraminifera host a variety of endosymbiont
49 partners (Decelle et al., 2015; Lee, 2006), which are thought to support early and adult life stages and
50 significantly contribute to total primary productivity (Kimoto, 2015). Still, foraminifera are omnivorous,
51 possibly even predominately carnivorous, with several studies suggesting that they can be effective preda-
52 tors (Anderson and Bé, 1976; Gaskell et al., 2019), mainly consuming live copepods (Caron and Be, 1984).
53 Radiolaria have several lineages, all of which have some taxa well known to host symbionts (Biard, 2022b).
54 Amongst Radiolarias, arguably the most widespread are Collodaria who can be either large solitary cells
55 or form massive colonies, up to several meters in length (Swanberg and Anderson, 1981). All known Col-
56 lodaria species host dinoflagellate symbionts (Biard, 2022b) and can contribute substantially to primary
57 productivity, particularly in oligotrophic ocean regions (Caron et al., 1995; Dennett et al., 2002). This
58 Collodaria-symbiont association has been suggested as a reason for their high abundances throughout the
59 photic zone of oligotrophic environments globally (Biard et al., 2017, 2016). A few Acantharea (Radiolaria
60 order) clades host algal symbionts (Biard, 2022b; Decelle et al., 2012), notably with two clades forming an
61 exclusive relationship with *Phaeocystis*. However, globally, Acantharea are less abundant than Collodaria
62 (Biard, 2022a) and contribute less to total primary productivity (Michaels et al., 1995). This may be due
63 to the fact several clades of Acantharea are cyst-forming and strictly heterotrophs (Biard, 2022b; Decelle et
64 al., 2013). Furthermore, Mars Brisbin et al. (2020) documented apparent predation behavior in Acantharea
65 near the surface, suggesting that there may be a larger reliance on carnivory.

66 Given the high abundances, yet diverse trophic strategies found among Rhizaria taxa, it is reasonable to
67 expect some form of niche partitioning. A number of studies do suggest evidence for vertical zonation
68 between Rhizaria groups according to various trophic strategies. Taxa-specific studies of Radiolarias suggest
69 they may be restricted to the euphotic zone (Boltovskoy, 2017; Michaels, 1988). Although some studies
70 report Acantharea in deeper waters (Decelle et al., 2013; Gutiérrez-Rodríguez et al., 2022), Phaeodarias,

71 alternatively, are generally found in the mesopelagic where photosynthesis cannot occur, but they can feed
72 on sinking particles (Stukel et al., 2018). In an imaging-based study of the whole Rhizaria community, Biard
73 and Ohman (2020) noted clear patterns in vertical zonation which largely corresponded to different trophic
74 roles. In the oligotrophic ocean, Blanco-Bercial et al. (2022) also noted that the protist community, including
75 Rhizaria, partition along an autotroph and mixotroph to heterotroph gradient with increasing depth in the
76 water column. Yet, few studies have made direct attempts to relate rhizaria abundances to environmental
77 factors (Biard and Ohman, 2020). In part, this is due to the fact few studies have been able to sample
78 Rhizaria in the same location over a consistent timeframe (Boltovskoy et al., 1993; Gutiérrez-Rodríguez et
79 al., 2022; Hull et al., 2011; Michaels et al., 1995; Michaels, 1988). Furthermore, no studies have utilized
80 imaging, arguably the best method for quantifying rhizaria, consistently throughout the full mesopelagic.
81 Given this lack of information, there are many unknowns with respect to Rhizaria ecology, seasonality and
82 phenology across different groups.

83 In this study, we present a comprehensive assessment of large Rhizaria measured for over a year from regularly
84 occurring cruises at monthly intervals. We utilized an in-situ imaging approach to facilitate abundance
85 calculations. With this dataset, we address two critical aims. 1) Quantification of large Rhizaria throughout
86 the epipelagic (0-200m) and mesopelagic (200-1000m) over the course of an annual cycle. These data were
87 collected in the Sargasso Sea, and represents the first study of its kind in an oligotrophic system; and 2) We
88 aim to test the hypothesis that Rhizaria exhibit niche partitioning according to trophic roles. This hypothesis
89 makes several predictions, including vertical zonation, as seen in prior studies, but also that environmental
90 variables related to trophic strategy will explain abundance patterns. Specifically, autotrophic/mixotrophic
91 taxa will correspond to variables related to autotrophy (chl-a concentration, primary productivity, local DO
92 maxima) and other rhizaria will correspond to factors which promote heterotrophy (particle concentration,
93 flux, and local DO minima).

⁹⁴ **Methods**

⁹⁵ **Oceanographic Sampling**

⁹⁶ Data were collected in collaboration with the Bermuda Atlantic Time-series Study (Lomas et al., 2013;
⁹⁷ Michaels and Knap, 1996) on board the R/V Atlantic Explorer. Cruises were conducted at approximately
⁹⁸ monthly intervals. Rhizaria individuals were sampled using the Underwater Vision Profiler 5 [UVP5; Picheral
⁹⁹ et al. (2010)], a tool which is well established to accurately quantify large Rhizaria (Barth and Stone, 2022;
¹⁰⁰ Biard et al., 2016; Biard and Ohman, 2020; Drago et al., 2022; Llopis Monferrer et al., 2022; Panaïotis
¹⁰¹ et al., 2023; Stukel et al., 2019; Stukel et al., 2018). The UVP5 was mounted to the sampling rosette
¹⁰² and collected data autonomously on routine casts, from which only the downcast data are utilized. The
¹⁰³ UVP5 was deployed from June-September 2019 then from October 2020 - January 2022, during which time
¹⁰⁴ the BATS region was sampled for 3-5 days at monthly intervals. Casts were filtered to only include data
¹⁰⁵ collected in the BATS region, far offshore of Bermuda in the Sargasso Sea (approximately 31.0°N-32.5°N,
¹⁰⁶ 64.25°W-63°W; Supplemental Figure 1). In general, casts extended to either 200m, 500m, or 1200m deep,
¹⁰⁷ with a few extended into the bathypelagic (4500m). However, Rhizaria were only typically found in large
¹⁰⁸ abundances throughout the epipelagic and mesopelagic zones. As such, we limit this study to results from
¹⁰⁹ the upper 1000m of the water column.

¹¹⁰ A variety of biotic and abiotic data were collected during each BATS cruise. Briefly, we will explain the data
¹¹¹ utilized in this study. The UVP5 provided particle count data at a high-frequency from each cast. Particle
¹¹² concentration was calculated from this data for all particles 184 μ m - 450 μ m. The lower size range was set
¹¹³ by what could be reliably sampled by the UVP5's pixel resolution (>2px; 0.092mm per pixel) and the upper
¹¹⁴ size range is representative of a potential prey field for mesozooplankton (Whitmore and Ohman, 2021). For
¹¹⁵ each UVP cast supporting continuous profiles of the CTD parameters salinity, temperature, and auxiliary

116 CTD channels; Dissolved Oxygen (DO), in-situ chlorophyll fluorescence were measured at 24Hz using the
117 BATS CTD package. On select casts, Niskin bottles were used to collect bacterial abundance estimates (via
118 epifluorescence microscopy) as well as measure inorganic nutrients (NO_3 , and Si as silicate/silicic acid) at
119 discrete depths. On each cruise, flux estimates of total mass, organic carbon, and nitrogen were also collected
120 using sediment traps; in the present study we utilized flux to the mesopelagic as the flux at 200m. Also
121 primary productivity was estimated through measuring ^{14}C uptake rates from in-situ incubations. For full
122 descriptions of the BATS sampling program and methods, see Knap et al. (1997) and Lomas et al. (2013)
123 for a review. Additionally, data can be viewed online (<https://bats.bios.asu.edu/bats-data/>).

124 Environmental data were processed in a variety of ways to match the format of the Rhizaria abundance
125 estimates (see below). CTD data were collected at higher frequency than the UVP (24Hz vs 15Hz respec-
126 tively), so these data were averaged within matching bins to the UVP5 data. Data from Niskin bottles were
127 first linearly interpolated in depth at 1m resolution then time averaged over the cruise, then subsequently
128 averaged into matching UVP5-sized bins. Primary productivity estimates were totaled within the euphotic
129 zone to represent a “total euphotic productivity”.

130 Rhizaria imaging processing and quantification

131 Individual vignettes of Rhizaria images were identified using the classification platform Ecotaxa (Picheral
132 et al., n.d.). Data were pre-sorted utilizing a random-forest classifier and pre-trained learning set. Taxo-
133 nomic classification were done based on morphology exclusively. While there are sparse taxonomic guides
134 for in-situ images of rhizaria, identification largely relied on descriptions in (Nakamura and Suzuki, 2015;
135 Suzuki and Not, 2015; and Biard and Ohman, 2020). Using the aforementioned sources and publicly avail-
136 able ecotaxa projects, we constructed a guide accessible at: https://thealexbarth.github.io/media//Project_
137 [Items/Oligotrophic_Community/ecotaxa_UVP-guide-stone-lab.pdf](#). Broadly, Rhizaria were classified as

138 Foraminifera, Radiolaria (Acantharea or Collodaria), or as a variety of Phaeodaria families (Figure 1).
139 When identification could not be confidently made between a few candidate taxa, a less specific label was
140 used. As a result, we have data from “unidentified Rhizaria”, which typically were vignettes not distinguish-
141 able between Aulacanthidae or Acantharea or “unidentified Phaeodaria”, which are clearly Phaeodaria but
142 not distinguishable into a family.

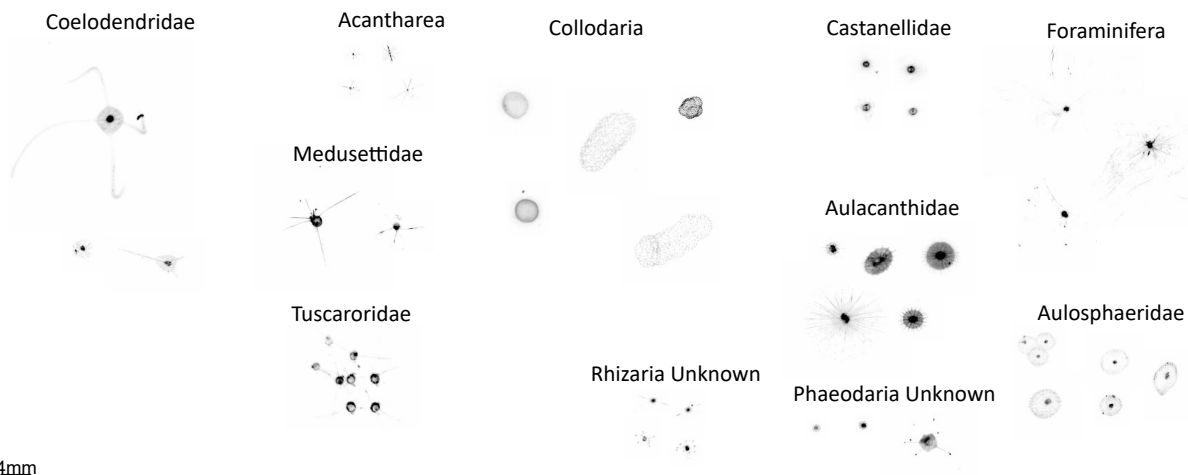


Figure 1: Example images of different Rhizaria taxa. 4mm scale bar shown in lower right. All vignettes are same scale

143 The UVP5 samples at \sim 15Hz rate as it descends the water column and records the exact position of each
144 particle larger than $600\mu m$. However, identified rhizaria ranged from a $934\mu m$ Aulacanthidae cell to a
145 Collodarian colony over 10mm in diameter. To confirm that the UVP5 was sampling adequately across
146 all size ranges, a normalized biomass size spectrum (NBSS) slope was constructed to identify a drop-off
147 which would indicate poor-sampling at the small size range (Barth and Stone, In press; Lombard et al.,
148 2019). However, it was evident from this analysis that all size ranges were adequately sampled across
149 the size range (Supplemental Figure 2) so no data were excluded. The UVP5 reports the exact depth at
150 which a particle is recorded, however to estimate abundance, observations must be binned over fixed depth

151 intervals. Our deployments had variable descent depths and speeds with more casts descending to 500m than
152 1000m and descents quicker through the epipelagic than the mesopelagic (see Barth and Stone (2022) for an
153 extended discussion of UVP5 data processing). For the present study, Rhizaria abundances were estimated
154 in 25m vertical bins, which offer a moderate sampling volume per bin (average $0.948m^3$ in the epipelagic
155 and $0.589m^3$ in the mesopelagic; Supplemental Table 1) while still maintaining ecologically relevant widths.
156 However, concentrations in a 25m bin would need to be greater than $2.428 \text{ ind. } m^{-3}$ and $3.912 \text{ ind. } m^{-3}$,
157 in the epipelagic and mesopelagic respectively, to fall below a 10% non-detection risk (Barth and Stone, In
158 press; Benfield et al., 1996). Because we typically observed many rhizaria taxa below these concentrations,
159 we present the 25m binned data to visualize broad-scale average distributions. For quantifying and modelling
160 Rhizaria abundances, we present integrated abundance estimates, with each cast. Due to the variable descent
161 depths of the UVP, data are categorized as epipelagic (0-200m), upper mesopelagic (200-500m), and lower
162 mesopelagic (500-1000m). The average sampling volume integrated through these regions were $7.59m^2$,
163 $7.06m^2$, and $11.77m^2$, with non-detection thresholds at $0.30 \text{ ind. } m^{-2}$, $0.33 \text{ ind. } m^{-2}$, and $0.20 \text{ ind. } m^{-2}$
164 respectively. All UVP data processing was done using the `EcotaxaTools` package in R (Barth 2023).

165 Modelling environmental controls of Rhizaria Abundance

166 Generalized Additive Models (GAMs) were used to assess the relationship between integrated Rhizaria abun-
167 dance and different environmental factors. GAMs offer the ability to model non-linear and non-monotonic
168 relationships, which can be particularly useful in assessing ecological relationships (Wood, 2017) and have
169 been successfully applied to Rhizaria ecology (Biard and Ohman, 2020). The `mgcv` package (Wood, 2001)
170 was used to construct models relating environmental parameters to each taxonomic group's integrated abun-
171 dance estimates from each cast. To select the most parsimonious model for each analysis, a backwards
172 step-wise approach was taken. First, a full model was fit using any term which may be ecologically relevant.

173 Terms were fit using maximum likelihood with a double penalty approach on unnecessary smooths (Marra
174 and Wood, 2011). The smoothness parameter was restricted ($k = 6$) to prevent overfitting the models. At
175 each iteration of the backwards step-wise procedure, the model term with the lowest F score (least statis-
176 tically significant) was removed. This was repeated until all model terms were statistically significant or
177 the R^2_{adj} was substantially reduced. Models were fit for each region; epipelagic, upper mesopelagic, and
178 lower mesopelagic. In cases where observations were too sparse for a given taxonomic grouping, models
179 were not run. All code and full models are available in code, as well as intermediate data products at
180 <https://github.com/TheAlexBarth/RhizariaSeasonality>.

181 Results

182 Environmental Variability

183 The BATS sampling region is southeast of Bermuda, situated in the oligotrophic North Atlantic Subtropical
184 Gyre. Due to the sampling location, while the environmental conditions are generally low in variation and
185 oligotrophic, there is considerable influence from deep winter-mixing and summer stratification as well as
186 secondary influences from mesoscale eddies which result in spatiotemporal heterogeneity (Lomas et al., 2013;
187 McGillicuddy et al., 1998). Variability in the water column structure was visible during the study period
188 (Figure 2). This is best evidenced through the temperature profiles; In the late summer and early fall
189 there was a stratified water column with high temperatures in the surface (<75m) (Figure 2A) and slightly
190 elevated salinity (Figure 2B). This warm, stratified period appeared more intense during the few months
191 sampled in 2019. In 2021, we observed the stratified layer slowly dissipated into the winter months following
192 mixed layer entrainment. There was a consistent oxygen minimum zone (OMZ) located at about 800m
193 deep (Figure 2C). February 2021 saw a notable downwelling event, likely due to a passing anti-cyclonic eddy

which impacted the local region during early 2021. During this phase, warmer, oxic water was significantly depressed deeper into the mesopelagic. This process was reversed in the spring months (March, April) primary due to the interaction of convective mixing and the passing of a strong cyclonic eddy resulting in a deep cold mixed layer. Primary production was highest during the spring mixing period, evidenced both by in-situ fluorescence (Figure 2D) and productivity incubation experiments (Figure 3A). Originating near the surface, the productivity peak moved deeper throughout the spring and declined into the summer (Figure 2D). However, there was a notable, yet smaller productivity bump in the late summer and early fall (Figure 3A) which occurred deeper in the epipelagic (Figure 2D). The particle concentration ($184\mu m - 450\mu m$) was closely coupled to chlorophyll-a patterns.

Overall, particle concentration was high near the surface during the 2021 spring bloom, then moved deeper throughout the water column attenuating throughout the lower epipelagic (Figure 2E). Similarly, heterotrophic bacteria abundance was closely linked to overall productivity, although there was a more consistent moderate-abundance layer near the top of the mesopelagic (~250m) (Figure 2F). Concurrent with the secondary fall production peak, there was also higher particle concentration and bacterial abundance in the later summer and early fall. Interestingly, while primary productivity estimates from July-August were not that different between 2019 and 2021 (Figure 3A), chlorophyll-a fluorescence, particle concentration, and bacterial abundance were much higher in 2019's summer/fall (Figure 2D-F). Inorganic nutrients (*Si* and NO_3) were generally well stratified, with low concentrations in the epipelagic and increasing throughout the mesopelagic. However, both nutrients did vary vertically in accordance with the 2021 February downwelling and spring mixing period (Figure 2G-H). Additionally, in the late fall of 2021, *Si* concentrations were slightly elevated in the mid-mesopelagic (Figure 2G).

Overall mass flux to the mesopelagic was highest during the 2021 February downwelling (Figure 3B). Generally, export was similarly high during March, declining in April then increasing slightly throughout the

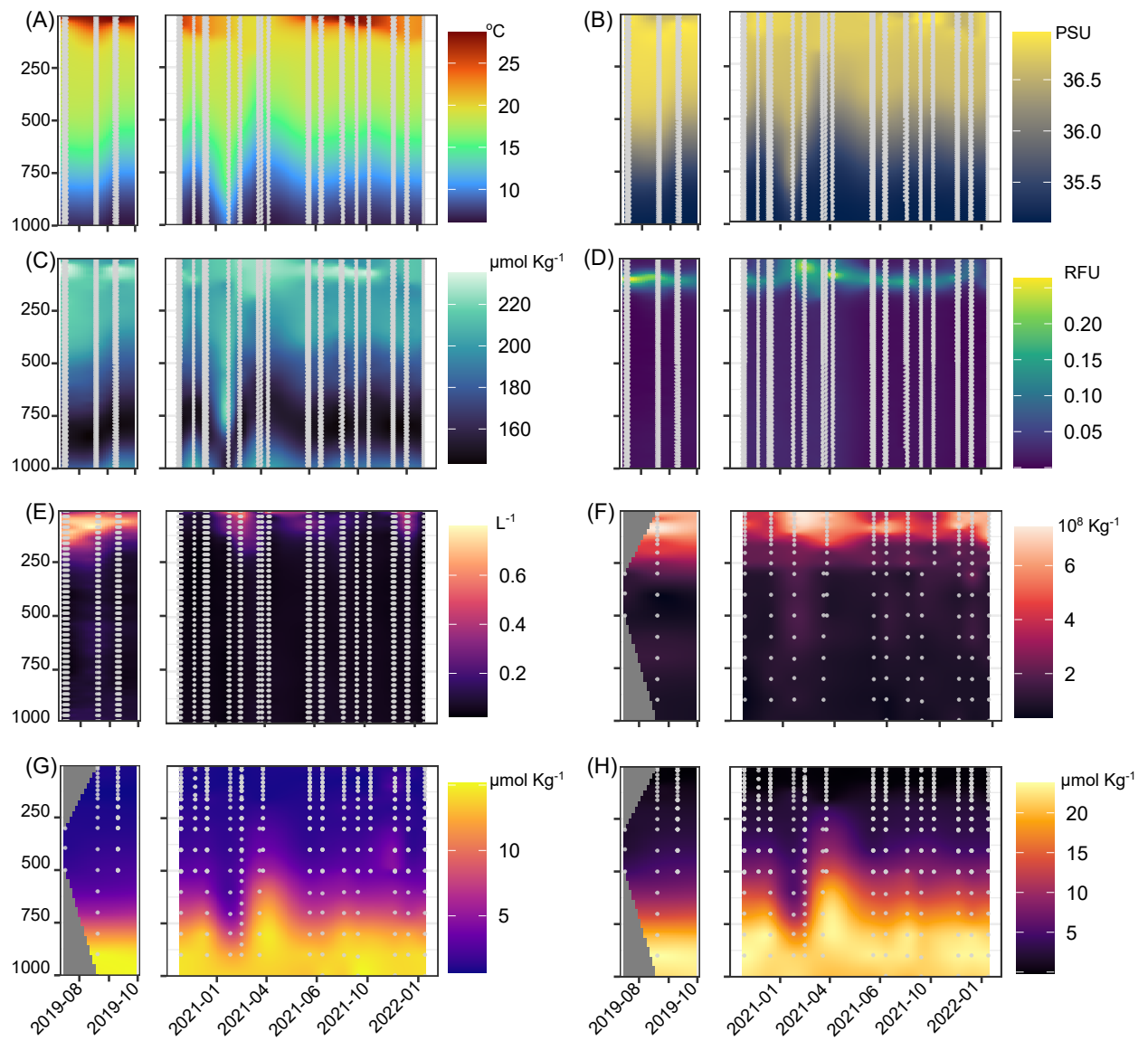


Figure 2: Environmental profiles across time-series of study period. Y axis shows depth in meters. (A) Temperature. (B) Salinity. (C) Dissolved Oxygen. (D) In-situ chlorophyll fluorescence. (E) Particle concentration ($184 - 450\mu\text{m}$). (F) Bacteria Abundance. (G) Silica. (H) Nitrate

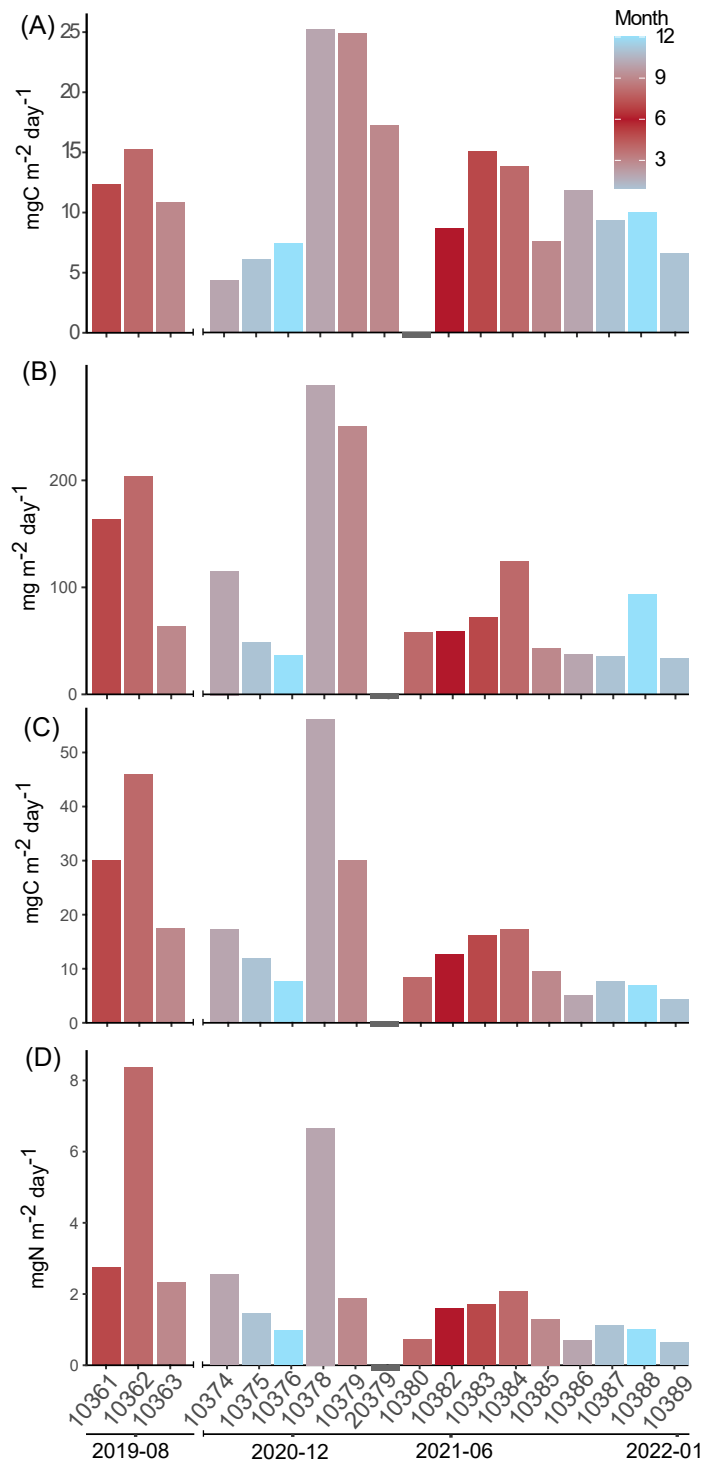


Figure 3: Primary productivity (A) and flux estimates from total mass (B), carbon (C), and nitrogen (D). Values are from monthly cruises with month displayed in corresponding colors. Absent data are shown by grey bar.

217 summer and early fall. While magnitude was slightly different, this pattern was consistent with total mass,
218 carbon and nitrogen fluxes (Figure 3B-D). Higher mass, carbon and nitrogen flux also occurred in the 2019
219 late summer - early fall period.

220 **Rhizaria abundance and distribution**

221 Across all imaged mesozooplankton ($>900\mu m$), Rhizaria comprised a considerable fraction of the total com-
222 munity. Considering the total abundances of the observational period, Rhizaria comprised on average, 42.6%
223 of all mesozooplankton abundance (Supplemental Figure 3). Copepods were the second most abundant, com-
224 prising 35.5% and all other living mesozooplankton were 22%. The large contribution of Rhizaria to the
225 mesozooplankton community is most prominent in the epipelagic, where they accounted for 47% of all meso-
226 zooplankton. In the mesopelagic rhizaria were a smaller (but still prominent fraction), at 38% in the upper
227 layers (200-500m) and 37% in the deeper mesopelagic (500-1000m).

228 Total average Rhizaria abundance had a bimodal distribution with respect to depth. Total abundance
229 was highest just below the surface (0-100m), with secondary, wider peak occurring in the mid mesopelagic
230 (Figure 4A). Variation in depth binned abundance was large, likely due to seasonal variability but also
231 increased from the detection-risk described in the methods. The vertical distribution pattern and abundance
232 varied considerably across taxonomic groups. Radiolarias were some of the most abundant taxa observed,
233 particularly in the epipelagic (Figure 4, Figure 5B). This pattern was led by Collodaria, whose colonies were
234 abundant in the upper epipelagic and declined into the top of the mesopelagic (Figure 4C). Acantharea
235 displayed a bimodal distribution accounting for a large portion of the total Rhizaria pattern (Figure 4B,
236 Figure 5). Foraminifera had a similar bimodal distribution, yet their overall average densities were much
237 lower and spread wider throughout the mesopelagic (Figure 4E). Phaeodaria families exhibited a wide range
238 of vertical distribution patterns. The most abundant, Aulacanthidae, also had a bimodal pattern but the

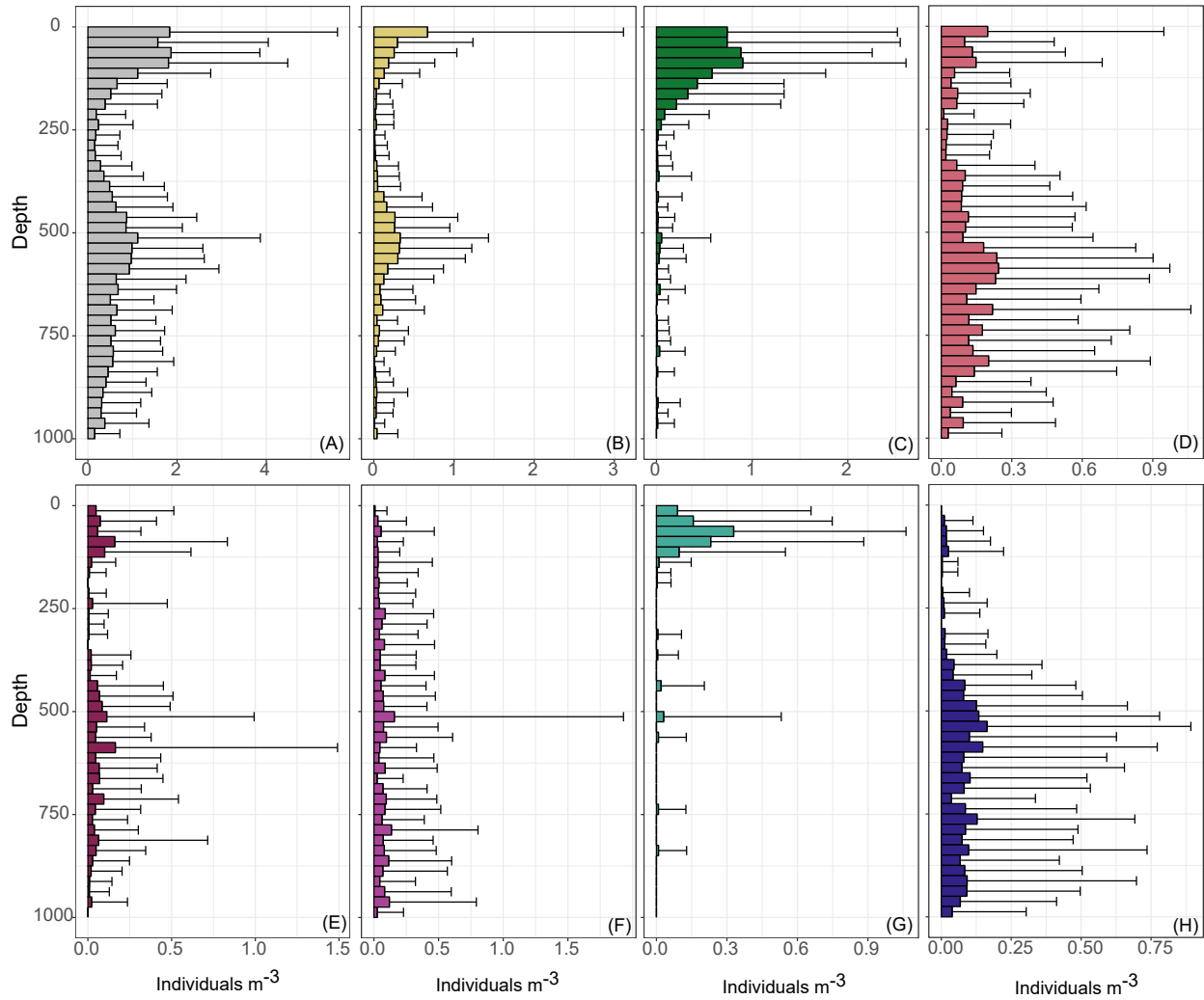


Figure 4: Average abundance of Rhizaria in 25m bins, across entire study period. Shown are total Rhizaria (A), Acantharea (B), Collodaria (C), Aulacanthidae (D), Foraminifera (E), Aulosphaeridae (F), Castanellidae (G), Coelodendridae (H).

density was highest in the lower mesopelagic (Figure 4D). Aulosphaeridae had low average density and was nearly homogeneously distributed throughout the water column, although slightly lower in the epipelagic (Figure 4F). Castanellidae were the only Phaeodaria who appeared to be effectively restricted to the photic zone (Figure 4G). Alternatively, Coelodendridae primarily occurred in the lower mesopelagic (Figure 4H). A few individuals from the families Tuscaroridae and Medusettidae were also observed in the mesopelagic, yet they were much rarer (data not shown).

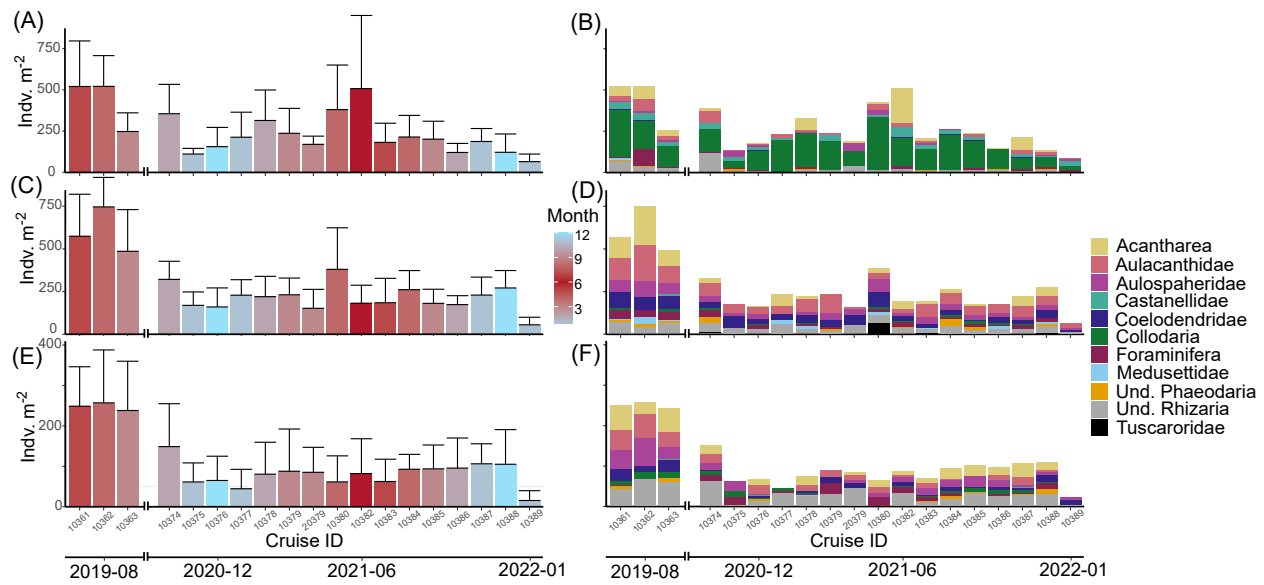


Figure 5: Seasonality of Rhizaria integrated abundance for the epipelagic (0-200m) (A-B), upper mesopelagic (200-500m) (C-D), lower mesopelagic (500-1000m) (E-F). Left panels (A,C,E) display total integrated abundance per monthly cruise colored by month. Right panels (B, D, F) display community composition of each total abundance.

Between the monthly cruises, Rhizaria integrated abundance varied in the epipelagic. Highest average abundance occurred in June 2021 and was lowest during the winter months (Figure 5A). The 2019 later summer - fall period also had much higher integrated abundance than similar months in 2021. While the majority of integrated abundance in the epipelagic was consistently attributable to Collodaria, Acanthrea abundance occurred sporadically and could account for a large portion of the total in some months (Figure

250 5B). The mesopelagic integrated abundance was much more consistent across monthly cruises, although
251 average abundance was notably higher in 2019 (Figure 5C-F). The community composition in the mesopelagic
252 was more diverse, mostly comprised of Phaeodarias. However, Acantharea and unidentified Rhizaria also
253 were common members of the community (Figure 5D, 5F).

254 **Body size throughout the water column.**

255 Very few taxa had consistent distributions throughout the water column. Only Acanthrea, Foraminifera,
256 Aulacanthidae, and Aulosphaeridae were consistently abundant in the epipelagic and mesopelagic. To in-
257 vestigate if the populations or morphologies shifted throughout the water column, we compared the sizes
258 (Equivalent Spherical Diameters, ESD) between mesopelagic and epipelagic groups for each taxa. All groups
259 were significantly different on average (Wilcox Rank Sum p-value <0.001). Acantharea were smaller, on
260 average in the mesopelagic while all other taxa tended to be larger (Figure 6).

261 **Environmental Drivers of Rhizaria Abundance**

262 For total Rhizaria integrated abundance the GAMs produced moderate fits ($R^2_{adj} = 0.406-0.603$) (Table 1). In
263 the epipelagic, there were several significant predictor variables including inorganic nutrients (NO_3 and Si),
264 water quality parameters (Salinity, DO), primary production, and particle concentration (Table 1). However,
265 the upper and lower mesopelagic were exclusively explained by particle-related variables (concentration and
266 mass flux) (Table 1).

Table 1: Generalized Additive Model results for integrated total Rhizaria abundance in different regions of the water column.

Model	Term	edf	F	p
All Rhizaria Epipelagic	Salinity	2.0818	4.654	<0.001

Model	Term	edf	F	p
$R^2_{adj} = 0.42$	DO	0.8272	0.945	0.0136
	Silica	3.1206	15.75	<0.001
	NO3	2.9970	6.268	<0.001
	Primary Productivity	1.8367	2.099	<0.001
	Particle Concentration	0.9282	2.566	<0.001
All Rhizaria Upper Mesopelagic	Silica	0.6847	0.431	0.073
$R^2_{adj} = 0.406$	Avg Mass Flux	1.5426	0.923	0.045
	Particle Concentration	3.2957	20.89	<0.001
All Rhizaria Lower Mesopelagic	Avg Mass Flux	1.6632	1.824	0.002
$R^2_{adj} = 0.603$	Particle Concentration	0.7694	0.662	0.027

267 GAMs for individual taxa were much less consistent in their fits (Table 2). This is likely in part due to
 268 the high number of non-observations for certain taxa. Note that due to low abundances, GAMs were not
 269 constructed for Tuscaroridae or Medusettidae. Furthermore no, significant terms were found for a model
 270 with Aulosphaeridae in the epipelagic nor Foraminifera in the mesopelagic.

271 Epipelagic Acantharea were explained by several predictor variables and had a good fit ($R^2_{adj} = 0.53$, Table
 272 2). Most notable smooths were mass flux and particle concentration, which had a weak positive association
 273 (Figure 7A), with July 2021 as a clear outlier where Acantharea abundances were high in the epipelagic
 274 despite lower fluxes and particle concentrations (Figure 5). Foraminifera had a good fitting GAM in the
 275 epipelagic ($R^2_{adj} = 0.445$). There were several significant explanatory variables, although the clearest pattern
 276 was observed of high temperatures associated with more Foraminifera abundance (Table 2, Figure 7B).

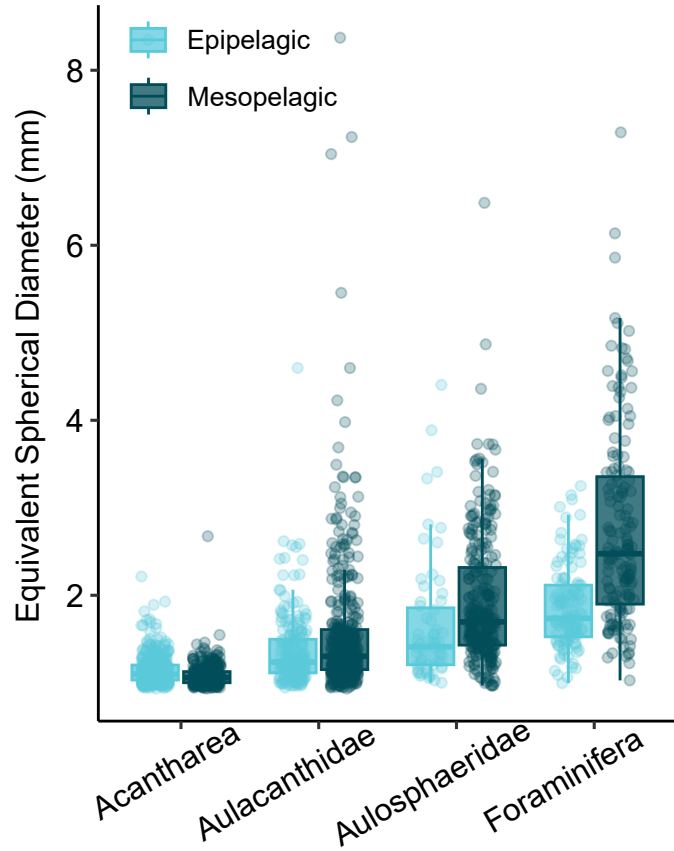


Figure 6: Comparison of average sizes (ESD) amongst Rhizaria taxa which occurred throughout the water column.

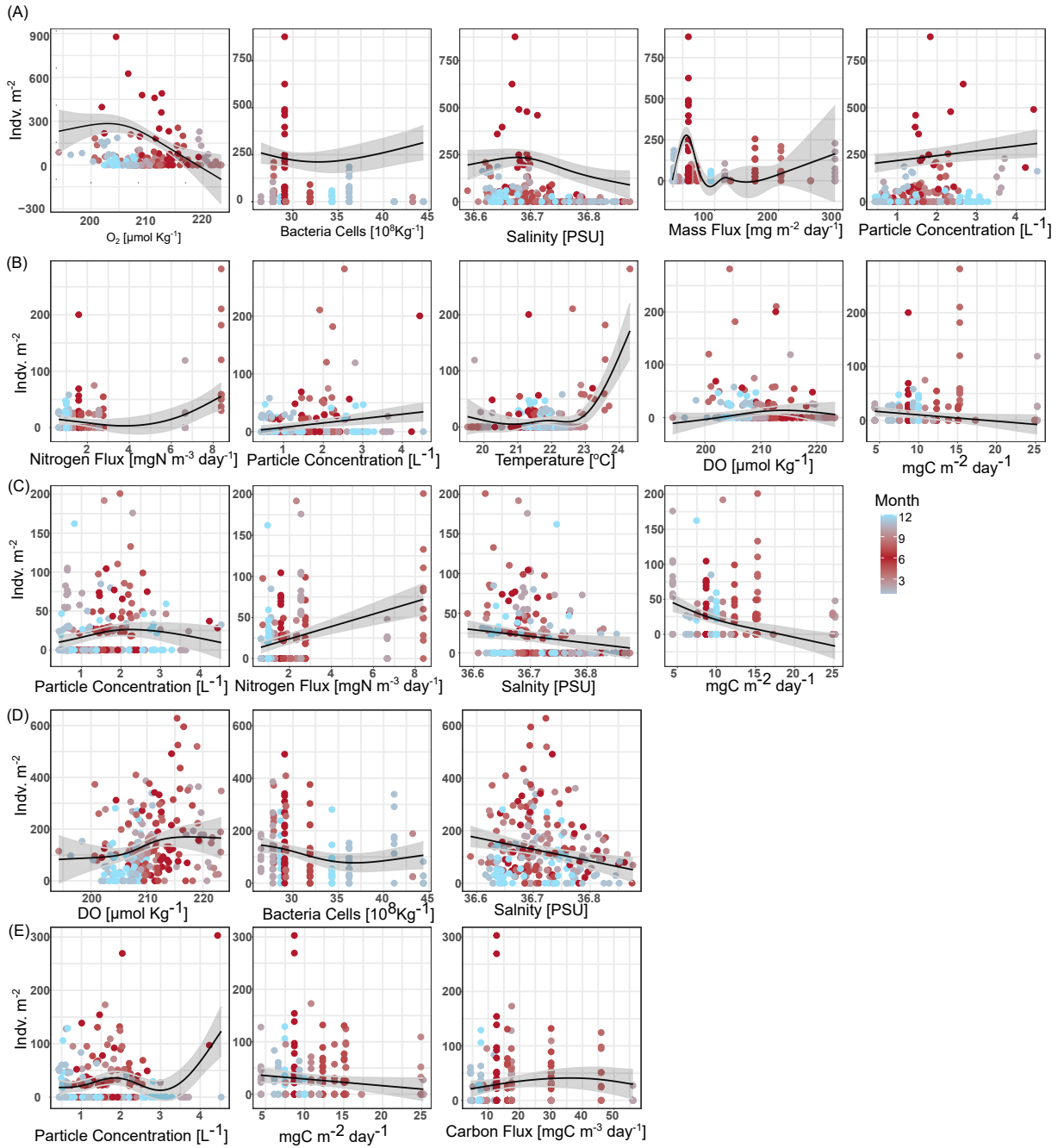


Figure 7: Partial effects of smooth terms in taxa-specific GAM models from the epipelagic (0–200m). Effects are grouped by taxa; Acantharea (A), Foraminifera (B), Aulacanthidae (C), Collodaria (D), Castanellidae (E).

277 Epipelagic Aulacanthidae similarly had several predictor variables which were significant, including both
 278 water quality parameters and particle/flux predictors (Table 2). Interestingly, Aulacanthidae had primary
 279 production as a significant predictor, yet there was not a clear association (Figure 7C). There was a fit
 280 for Collodaria in the epipelagic ($R^2_{adj} = 0.16$), although there was a logit-like relationship where higher
 281 abundances tended to occur during higher DO conditions in the surface waters (Figure 7D). Castanellidae
 282 also had similarly poor fits in the epipelagic ($R^2_{adj} = 0.124$) (Table 2, Figure 7E).

Table 2: Taxa-specific generalized additive models for different regions of the water column.

Model	Term	edf	F	p
Acantharea Epipelagic	Salinity	2.264	4.113	<0.001
R2adj=0.53	O2	2.579	6.712	<0.001
	Avg Mass Flux	4.810	22.81	<0.001
	Bacteria #/L	1.599	1.317	0.0117
	Particle Concentration	0.853	1.158	0.0087
Acantharea Upper Mesopelagic	Avg C Flux	1.296	0.621	0.0439
R2adj=0.231	Avg N Flux	1.619	1.283	0.0026
	Particle Concentration	0.952	3.886	<0.001
Acantharea Lower Mesopelagic	Temperature	2.076	4.155	<0.001
R2adj=0.509	Avg N Flux	1.494	1.216	0.0113
	Primary Productivity	0.766	0.648	0.0253
	Particle Concentration	2.037	10.03	<0.001
Aulacanthidae Epipelagic	Salinity	0.792	0.757	0.0241
R2adj=0.251	Avg N Flux	0.869	1.324	0.0018

Model	Term	edf	F	p
	Primary Productivity	2.312	7.704	<0.001
	Particle Concentration	2.008	2.200	0.0017
Aulacanthidae Upper Mesopelagic	Particle Concentration	2.832	9.802	<0.001
R2adj = 0.158				
Aulacanthidae Lower Mesopelagic	Avg Mass Flux	1.622	1.991	0.002
R2adj=0.298	Particle Concentration	2.123	6.706	<0.001
Aulosphaeridae Upper Mesopelagic	Particle Concentration	2.653	13.06	<0.001
R2adj=0.2				
Aulosphaeridae Lower Mesopelagic	Particle Concentration	0.972	6.248	<0.001
R2adj=.147				
Castanellidae Epipelagic	Avg C Flux	1.462	0.816	0.0421
R2adj = 0.124	Primary Productivity	0.771	0.665	0.0247
	Particle Concentration	3.956	4.623	<0.001
Coelodendridae Upper Mesopelagic	Avg N Flux	0.822	0.919	0.0183
R2adj=.113	Particle Concentration	0.970	6.208	<0.001
Coelodendridae Lower Mesopelagic	Particle Concentration	1.773	4.873	<0.001
R2adj=.133				
Collodaria Epipelagic	Salinity	0.925	2.267	<0.001
R2adj=0.16	O2	2.015	2.217	0.002
	Bacteria #/L	1.843	2.100	0.002
Foraminifera Epipelagic	Temperature	4.414	8.789	<0.001
R2adj=0.445	O2	1.603	1.287	0.0111

Model	Term	edf	F	p
	Avg N Flux	2.512	3.396	<0.001
	Primary Productivity	0.824	0.920	0.0153
	Particle Concentration	0.919	2.257	<0.001

283 In the upper mesopelagic (200-500m), abundances were generally low (Figure 4) so GAMs were only con-
 284 structed for Acantharea, Aulacanthidae, Aulosphaeridae, and Coelodendridae (Table 2). All these models
 285 had generally poor fits ($R^2_{adj} < 0.25$). Yet, for all upper mesopelagic models, particle concentration was a
 286 significant explanatory variable (Table 2, Figure 8). Carbon flux was significant for Acantharea and nitrogen
 287 flux was significant for both Acantharea and Coelodendridae (Table 2, Figure 8A,D). The lower mesopelagic
 288 also had generally poor GAM fits for taxa specific models ($R^2_{adj} < 0.3$), with the exception of Acantharea
 289 ($R^2_{adj} = 0.509$). Acantharea in the lower mesopelagic was most clearly positively associated with particle
 290 concentration and nitrogen flux, as well as temperature to a slight degree (Figure 9A). For all Phaeodarias
 291 with a significant model, particle concentration was a main predictor variable (Table 2, Figure 9B-D). Aula-
 292 canthidae had the best fitting model of the Phaeodarias ($R^2_{adj} = 0.298$), which also included mass flux as a
 293 statistically significant smooth (Figure 9B).

294 Discussion

295 Overall Rhizaria abundance and patterns

296 In the epipelagic Rhizaria exhibited a notable seasonal pattern. Rhizaria abundances were higher in the
 297 summer months and lower during the winter. During a prior time period, Blanco-Bercial et al. (2022) noted
 298 that there is considerable seasonality in the community composition of all protists. Despite the seasonality

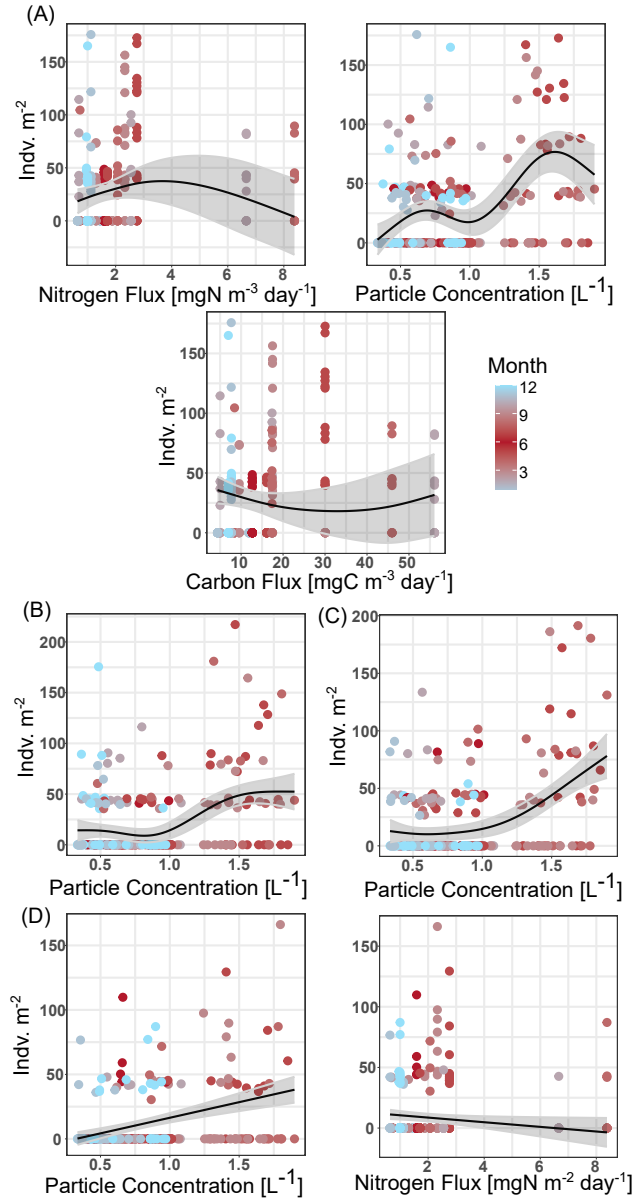


Figure 8: Partial effects of smooth terms in taxa-specific GAM models from the upper mesopelagic (200–500m). Effects are grouped by taxa; Acantharea (A), Aulacanthidae (B), Aulosphaeridae (C), Coelodendridae (D).

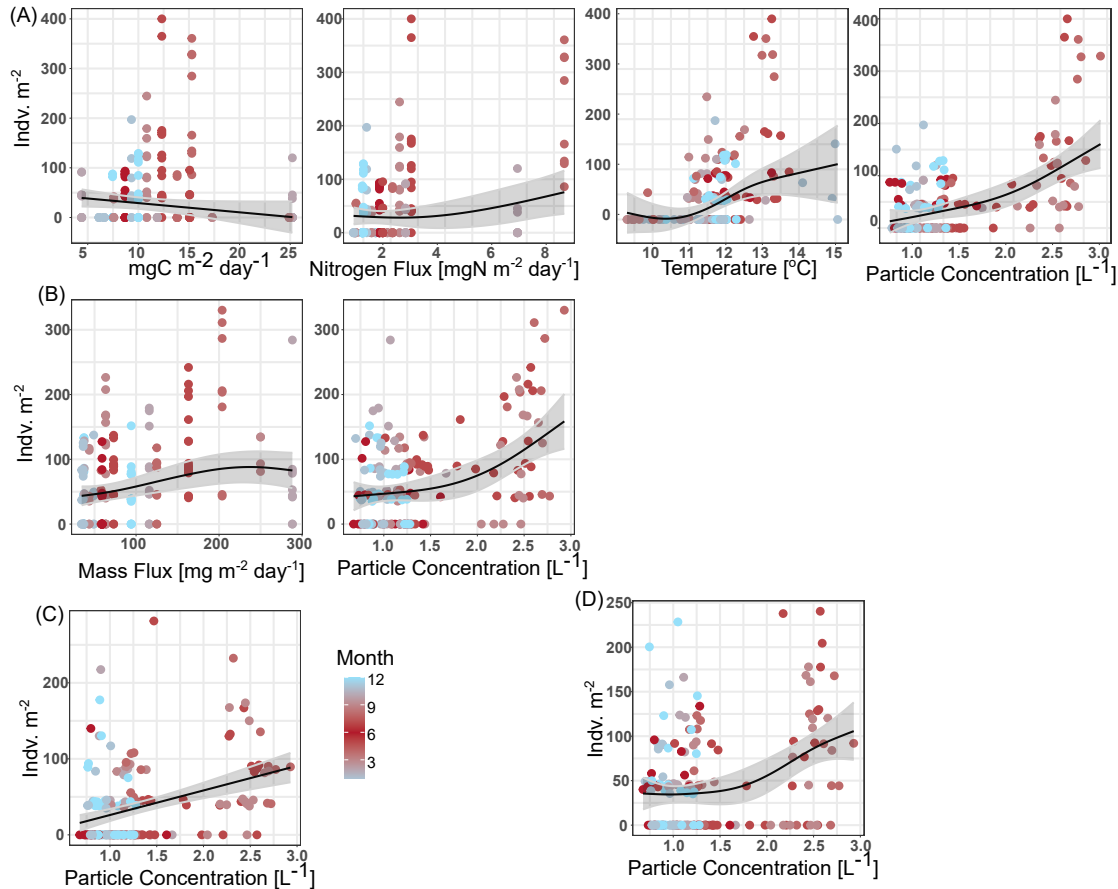


Figure 9: Partial effects of smooth terms in taxon-specific GAM models from the lower mesopelagic (500–1000m). Effects are grouped by taxa; Acantharea (A), Aulacanthidae (B), Aulosphaeridae (C), Coelodendriidae (D).

299 of total Rhizaria abundance, community composition was relatively consistent, with Collodaria representing
300 the bulk of the community. It should be noted that the overall taxonomic resolution of the UVP5 is fairly
301 low, so there may be a switching of species within the broad groups identified in this study which were not
302 captured. Throughout the mesopelagic, month-to-month variation in 2021 was relatively low. Again, this is
303 consistent with observations from metabarcoding of the whole protist community in the same study region
304 (Blanco-Bercial et al., 2022). This finding is not surprising as the overall seasonal variation in environmental
305 conditions in this region were low.

306 Overall Rhizaria were the most commonly identified group of mesoplankton throughout the study period.
307 We do note that the UVP5 commonly captures *Trichodesmium* colonies, yet these were excluded in this
308 comparison as they are strictly autotrophs. It should be noted that previous work has suggested that
309 avoidance behavior with the UVP is possible, at times likely, for visual and highly mobile zooplankton
310 (Barth and Stone, 2022). Thus, the percent contribution reported here (42.7%) of Rhizaria to the total
311 mesozooplankton community may be inflated due to under sampling of organisms such as Euphausiids and
312 Chaetognaths which have quick escape responses. Regardless, it is worth noting that in the same region,
313 with data collected in 2012 and 2013 using similar calculation methods, Biard et al. (2016) estimated
314 Rhizaria only contribute 15% of the total mesozooplankton community in the upper 500m. Likely, Rhizaria
315 display considerable interannual variability. In the present study, we noticed considerably higher Rhizaria
316 abundance throughout the water column in 2019 compared to 2021. While this may have been driven by
317 increased mass flux, more information is needed to truly understand the magnitude by which Rhizaria can
318 vary interannually.

319 **Relationship to environmental parameters**

320 In general, the fit of most GAMs were moderate to poor. One possible reason for the poor fits may have
321 been that for some taxa, conditions were not variable enough to capture a range of conditions at which
322 they may exist. For instance, Collodaria were the most abundant taxa observed, yet the fit of their GAM
323 was particularly poor. In studies which covered a wider range of parameters, Collodaria has been shown
324 to strongly vary with changes in parameters such as temperature, chlorophyll-a, mixing, and water clarity
325 (Biard et al., 2017; Biard and Ohman, 2020). Alternatively, Acantharea had relatively good fitting GAMs.
326 These taxa also had some of the largest variation from month to month on cruises. Thus, it may be that
327 in the oligotrophic, the relatively stable conditions can support certain taxa while others are more sporadic.
328 It should also be noted that due to the challenge of adequately sampling enough volume to overcome low-
329 detection issues, GAMs were run on integrated data. However, variation with environmental parameters
330 throughout the water column are likely, just not captured in the modelling aspect of this study. One
331 consistent parameter which had significant positive associations was particle concentration. This observation
332 is not surprising as most rhizaria likely to some extent engage in flux feeding.

333 **Vertical Structure and Trophic Roles**

334 In this study we present a clear pattern of vertical zonation between different Rhizaria groups. Largely, the
335 taxonomic composition and vertical positioning were similar to Rhizaria zonation in the California Current
336 Ecosystem (Biard and Ohman, 2020). It should be noted however, that the secondary abundance peak
337 reported in the present study is lower. This is likely due to the more oligotrophic nature of the study region,
338 were the euphotic zone penetrates deeper into the water column. Most prevalent in the epipelagic were
339 Collodaria. These mixotrophic Radiolarians have long been reported to contribute to primary productivity
340 in the euphotic zone (Dennett et al., 2002; Michaels et al., 1995). Collodaria are thought to be particularly

341 successful globally in oligotrophic regions due to their photosymbiotic relationships (Biard et al., 2017, 2016).
342 We observed the highest abundance of Collodaria during June 2021, supporting the notion they can thrive
343 during the typically low-nutrient conditions of summer stratification. However, Collodaria also increased
344 during the spring mixing period, suggesting that they can thrive during conditions which may typically be
345 thought to favor autotrophs. Furthermore, while Collodaria were primarily absent from below 250m, there
346 were a few instances of deeper colonies being observed. Global investigations of polycystine flux, suggest
347 that deep-Collodaria in Oligotrophic regions may be a consequence of isothermal submersion (Boltovskoy,
348 2017). Alternatively, surface waters at BATS often mix into the mode water during the seasonal mixing,
349 so Collodaria in the deeper waters may be a result of diapycnal mixing. Another effectively exclusively
350 epipelagic Rhizaria was the Phaeodaria family of Castanellidae. All Phaeodaria are thought to be fully
351 heterotrophic (Nakamura and Suzuki, 2015), nonetheless a number of studies, including this one, report
352 Castanellidae to be typically found in the lower epipelagic (Biard et al., 2018; Biard and Ohman, 2020;
353 Zasko and Rusanov, 2005). It should be considered that perhaps Castanellidae specializes in feeding on
354 sinking particles directly at the base of the epipelagic. Given it's smaller size (Nakamura and Suzuki, 2015),
355 Castanellidae does not need a large diameter to efficiently flux feed at the typically particle rich region of the
356 lower epipelagic. Both Castanellidae and Collodaria had poor fitting GAMs. This is somewhat of a surprise
357 for Collodaria who had large abundance. However, given the consistency of their abundance, it may be that
358 this study did not capture a wide enough range of conditions for describing Collodaria's preferred niche.

359 The mesopelagic generally was home to known heterotrophic organisms, particularly for those which were
360 constrained to exclusively occupy deeper waters. This is consistent with Blanco-Bercial et al. (2022)'s
361 observation of an auto-/mixotroph to heterotroph gradient in the protist community. The upper mesopelagic
362 interestingly had relatively low total abundance. This low-abundance region likely reflects the dynamics of
363 productivity and export throughout the water column. While productivity and thus sinking particles for

364 flux feeders are high in the euphotic zone, much of this is attenuated throughout the epipelagic. So, while
365 the base of the epipelagic may provide a rich feeding environment for Castanellidae, smaller protists, or
366 heterotrophic bacteria (Figure 2F), the region from 200-500m might be otherwise food poor. Perhaps it is
367 more advantageous for Rhizaria to situate deeper, in darker regions of the twilight zone. Also it should be
368 noted that Phaeodaria utilize silica to build their opaline tests, and silica concentrations started to increase
369 around 500m (Figure 2G). Although *Si* was not a significant smooth for any taxa-specific model, this lack
370 of association might be due to the overall lack of variation of *Si* between integrated abundance of each cast.
371 Aulosphaeridae was only found to have significant relationships, although weak fits, to particle concentration
372 in the mesopelagic. In our study, while consistently observed, overall abundances of Aulosphaeridae were
373 very low. In the Pacific Ocean, on California's Coast, much higher abundances of Aulosphaeridae have been
374 reported (Biard and Ohman, 2020; Zasko and Rusanov, 2005) and they have massive potential to impact
375 silica export (Biard et al., 2018). Coelodendridae were also seemingly restricted to the deeper section of
376 the mesopelagic. This is interesting given that in the California Current, (Biard and Ohman, 2020) found
377 a bimodal distribution in Coelodendridae. There are several morphotypes corresponding to different taxa
378 of Coelodendridae (Biard and Ohman, 2020; Nakamura and Suzuki, 2015). So it may be that only a few
379 types of Coelodendridae were observed in this study, while the epipelagic variety was not. Alternatively, the
380 lower epipelagic of the California Current may provide adequate habitat for Coelodendridae, which is not
381 available in the oligotrophic Sargasso Sea.

382 A number of taxa were found to have a bimodal distribution, with considerable populations in both the
383 epipelagic and mesopelagic. Aulacanthidae had a bimodal distribution, although abundances were highest
384 in the lower mesopelagic. Foraminifera also had a bimodal distribution. Some lineages of Foraminifera
385 are known to host photosymbionts (Biard, 2022a; Kimoto, 2015), however they are also efficient predators
386 commonly seen throughout the mesopelagic (Caron and Be, 1984; Gaskell et al., 2019). Thus it is not

surprising to find their presence in both locations of the water column. Foraminifera are also known to vary their vertical distribution across their life cycle in phase with lunar cycles (Biard, 2022a; Bijma et al., 1990; Gaskell et al., 2019; Kimoto, 2015). However, the sampling scheme of the BATS program does not capture this frequency and was not investigated in the present study.

Acantharea also had a bimodal distribution, with much larger abundances than Aulacanthidae or Foraminifera. Most prior studies of Acantharea vertical distribution found them concentrated in near surface layers of the water column Zasko and Rusanov (2005). This would support the paradigm that large Acantharea abundances may be supported by their mixotrophic abilities (Michaels et al., 1995; Suzuki and Not, 2015). While the UVP5 images cannot distinguish between mixotrophic and heterotrophic Acantharea, the GAMs constructed for Acantharea abundance found positive associations with particle concentration and mass flux, suggesting a higher reliance on heterotrophy. Recently Mars Brisbin et al. (2020) described apparent predator behavior amongst near-surface Acantharea. Thus it is likely that epipelagic Acantharea may commonly be heterotrophic. Yet, it should be noted in the Sargasso Sea, both heterotrophic and symbiotic lineages of Acantharea have been reported (Blanco-Bercial et al., 2022). Additionally, Michaels (1988) noted that the majority of Acantharea (by abundance) were smaller than $160\mu m$. While that estimate may be inflated due to inability to capture larger cells, small Acantharea were not captured in the present study. Thus, trophic strategy may shift based on sizes of Acantharea.

Decelle et al. (2013) proposed a hypothetical life cycle for cyst-bearing (strictly heterotrophic) Acantharea. This hypothesized life cycle suggests that epipelagic Acantharea are adult populations, which form cysts that sink into the mesopelagic, then reproduce and rise. Furthermore, given that horizontal transfer of symbionts between generations of Acantharea is unlikely due to their spawning behavior, the newly spawned mesopelagic Acantharea are not necessarily required to rapidly return to the photic zone (Decelle et al., 2013, 2012). This hypothesis predicts that Acanthareas in the mesopelagic would be smaller (Decelle et al.,

410 Mars Brisbin et al. (2020) provided some support for this hypothesis, with a significant decrease
411 in Acantharea sizes with depth. Although the authors also observed low abundances in the mesopelagic
412 and noted that the smaller sizes may be due to lower food availability (Mars Brisbin et al., 2020). Since
413 food is more scarce in the mesopelagi, nutritional quality lower, yet flux feeders would likely grow larger to
414 increase their feeding range (Biard and Ohman, 2020). In the data collecting in this study, Acanthareas in
415 the mesopelagic were significantly smaller than the epipelagic, despite the other bimodal taxa (Foraminifera
416 and Aulacanthidae) being significantly larger with depth. This provides added support for the hypothesis
417 that cyst-forming Acantharea may utilize different sections of the water column throughout their life cycle.
418 However to further investigate this, more work is needed with higher temporal and taxonomic resolution.

419 **Conclusions and Considerations**

420 This study provides a detailed look at Rhizaria abundance over time throughout the water column in a major
421 oligotrophic gyre. We show that their abundances are generally related to particle concentration and flux,
422 although lack of environmental variability may have reduced the fit of our GAMs. Considering the potential
423 role of Rhizaria in the biological carbon pump, they may have a somewhat mixed role. In the shallower
424 regions, where smaller Rhizaria are abundant, they may be an attenuating force on sinking particles (Stukel
425 et al., 2019). It should be noted that in our study, we focused on the “small” particle concentration field
426 ($<450\mu m$), and these particles are generally slower sinking than large particles. However, once consumed and
427 repackaged by larger Rhizaria, they can sink quicker and contribute more to overall flux (Michaels, 1988).
428 Thus, Rhizaria may act as an aggregation mechanism. However, this is largely speculation, to truly test this,
429 more work is needed measuring Rhizaria flux.

430 The vertical partitioning documented in this study do support the hypothesis that mixotrophic rhizaria will
431 occupy shallower waters while deeper waters are dominated by heterotrophy. However the degree to which

432 mixotrophic Rhizaria in the euphotic zone rely on heterotrophy versus symbiosis is uncertain. Collodaria were
433 recorded as consistent and dominant members of the near surface region. These organisms have the potential
434 to contribute considerably to the otherwise low productivity of oligotrophic regions. However, their role in
435 food webs is not well understood. While this study represents a step-forward in our understanding of Rhizaria
436 ecology, continued research on Rhizaria is much needed to better understand their ecology. Particularly
437 extended descriptive work to capture interannual patterns. Also work defining biotic interactions, feeding
438 rates, productivity, and life history are all rich fields of interest in Rhizaria.

439 **References:**

- 440 Anderson, O.R., 2014. Living Together in the Plankton: A Survey of Marine Protist Symbioses. *Acta*
441 *Protozoologica* 53, 29–38. <https://doi.org/10.4467/16890027AP.13.0019.1116>
- 442 Anderson, O.R., Bé, A.W.H., 1976. A CYTOCHEMICAL FINE STRUCTURE STUDY OF PHAGOTRO-
443 PHY IN A PLANKTONIC FORAMINIFER, *HASTIGERINA PELAGICA* (d'ORBIGNY). *The Biolog-*
444 *ical Bulletin* 151, 437–449. <https://doi.org/10.2307/1540498>
- 445 Aurahs, R., Grimm, G.W., Hemleben, V., Hemleben, C., Kucera, M., 2009. Geographical distribution of
446 cryptic genetic types in the planktonic foraminifer *Globigerinoides ruber*. *Molecular Ecology* 18, 1692–
447 1706. <https://doi.org/10.1111/j.1365-294X.2009.04136.x>
- 448 Barth, A., Stone, J., In press. Understanding the picture: The promises and challenges of in-situ imagery data
449 in the study of plankton ecology. *Journal of Plankton Research: Horizons*.
- 450 Barth, A., Stone, J., 2022. [Comparison of an in situ imaging device and net-based method to study meso-](#)
451 [zooplankton communities in an oligotrophic system](#). *Frontiers in Marine Science* 9.
- 452 Benfield, M.C., Davis, C.S., Wiebe, P.H., Gallager, S.M., Gregory Lough, R., Copley, N.J., 1996. Video
453 Plankton Recorder estimates of copepod, pteropod and larvacean distributions from a stratified region

- 454 of Georges Bank with comparative measurements from a MOCNESS sampler. Deep Sea Research Part
455 II: Topical Studies in Oceanography 43, 1925–1945. [https://doi.org/10.1016/S0967-0645\(96\)00044-6](https://doi.org/10.1016/S0967-0645(96)00044-6)
- 456 Biard, T., 2022a. Rhizaria. Encyclopedia of Life Sciences, pp. 1–11. <https://doi.org/10.1002/9780470015902.a0029469>
- 457
- 458 Biard, T., 2022b. Diversity and ecology of Radiolaria in modern oceans. Environmental Microbiology 24,
459 2179–2200. <https://doi.org/10.1111/1462-2920.16004>
- 460 Biard, T., Bigeard, E., Audic, S., Poulain, J., Gutierrez-Rodriguez, A., Pesant, S., Stemmann, L., Not, F.,
461 2017. Biogeography and diversity of Collodaria (Radiolaria) in the global ocean. The ISME Journal 11,
462 1331–1344. <https://doi.org/10.1038/ismej.2017.12>
- 463 Biard, T., Krause, J.W., Stukel, M.R., Ohman, M.D., 2018. The Significance of Giant Phaeodarians
464 (Rhizaria) to Biogenic Silica Export in the California Current Ecosystem. Global Biogeochemical Cy-
465 cles 32, 987–1004. <https://doi.org/10.1029/2018GB005877>
- 466 Biard, T., Ohman, M.D., 2020. Vertical niche definition of test-bearing protists (Rhizaria) into the twilight
467 zone revealed by in situ imaging. Limnology and Oceanography 65, 2583–2602. <https://doi.org/10.1002/lno.11472>
- 468
- 469 Biard, T., Pillet, L., Decelle, J., Poirier, C., Suzuki, N., Not, F., 2015. Towards an integrative morpho-
470 molecular classification of the collodaria (polycystinea, radiolaria). Protist 166, 374–388. <https://doi.org/10.1016/j.protis.2015.05.002>
- 471
- 472 Biard, T., Stemmann, L., Picheral, M., Mayot, N., Vandromme, P., Hauss, H., Gorsky, G., Guidi, L., Kiko,
473 R., Not, F., 2016. In situ imaging reveals the biomass of giant protists in the global ocean. Nature 532,
474 504–507. <https://doi.org/10.1038/nature17652>
- 475 Bijma, J., Erez, J., Hemleben, C., 1990. **Lunar and semi-lunar reproductive cycles in some spinose planktonic**
476 **foraminifers.** Journal of Foraminiferal Research 20, 117–127.

- 477 Blanco-Bercial, L., Parsons, R., Bolaños, L.M., Johnson, R., Giovannoni, S.J., Curry, R., 2022. [The pro-](#)
- 478 [tist community traces seasonality and mesoscale hydrographic features in the oligotrophic sargasso sea.](#)
- 479 Frontiers in Marine Science 9.
- 480 Boltovskoy, D., 2017. Vertical distribution patterns of radiolaria polycystina (protista) in the world ocean:
- 481 Living ranges, isothermal submersion and settling shells. Journal of Plankton Research 39, 330–349.
- 482 <https://doi.org/10.1093/plankt/fbx003>
- 483 Boltovskoy, D., Alder, V.A., Abelmann, A., 1993. Annual flux of radiolaria and other shelled plankters in
- 484 the eastern equatorial atlantic at 853 m: seasonal variations and polycystine species-specific responses.
- 485 Deep Sea Research Part I: Oceanographic Research Papers 40, 1863–1895. [https://doi.org/10.1016/0967-0637\(93\)90036-3](https://doi.org/10.1016/0967-0637(93)90036-3)
- 486 Caron, D.A., 2016. [The rise of rhizaria | nature](#). Nature 532, 444–445.
- 487 Caron, D.A., Be, A.W.H., 1984. PREDICTED AND OBSERVED FEEDING RATES OF THE SPINOSE
- 488 PLANKTONIC FORAMINIFER. BULLETIN OF MARINE SCIENCE 35.
- 489 Caron, D.A., Michaels, A.F., Swanberg, N.R., Howse, F.A., 1995. Primary productivity by symbiont-bearing
- 490 planktonic sarcodines (acantharia, radiolaria, foraminifera) in surface waters near bermuda. Journal of
- 491 Plankton Research 17, 103–129. <https://doi.org/10.1093/plankt/17.1.103>
- 492 Cavalier-Smith, T., Chao, E.E., Lewis, R., 2018. Multigene phylogeny and cell evolution of chromist infrak-
- 493 ingdom Rhizaria: contrasting cell organisation of sister phyla Cercozoa and Retaria. Protoplasma 255,
- 494 1517–1574. <https://doi.org/10.1007/s00709-018-1241-1>
- 495 Cohen, N.R., Krinos, A.I., Kell, R.M., Chmiel, R.J., Moran, D.M., McIlvin, M.R., Lopez, P.Z., Barth, A.,
- 496 Stone, J., Alanis, B.A., Chan, E.W., Breier, J.A., Jakuba, M.V., Johnson, R., Alexander, H., Saito, M.A.,
- 497 2023. Microeukaryote metabolism across the western North Atlantic Ocean revealed through autonomous
- 498 underwater profiling. <https://doi.org/10.1101/2023.11.20.567900>

- 500 Decelle, J., Colin, S., Foster, R.A., 2015. Photosymbiosis in Marine Planktonic Protists, in: Ohtsuka, S.,
501 Suzuki, T., Horiguchi, T., Suzuki, N., Not, F. (Eds.), Springer Japan, Tokyo, pp. 465–500. https://doi.org/10.1007/978-4-431-55130-0_19
- 502
- 503 Decelle, J., Martin, P., Paborstava, K., Pond, D.W., Tarling, G., Mahé, F., De Vargas, C., Lampitt, R.,
504 Not, F., 2013. Diversity, Ecology and Biogeochemistry of Cyst-Forming Acantharia (Radiolaria) in the
505 Oceans. PLoS ONE 8, e53598. <https://doi.org/10.1371/journal.pone.0053598>
- 506 Decelle, J., Siano, R., Probert, I., Poirier, C., Not, F., 2012. Multiple microalgal partners in symbiosis
507 with the acantharian *Acanthochiasma* sp. (Radiolaria). Symbiosis 58, 233–244. <https://doi.org/10.1007/s13199-012-0195-x>
- 508
- 509 Dennett, M.R., Caron, D.A., Michaels, A.F., Gallager, S.M., Davis, C.S., 2002. Video plankton recorder
510 reveals high abundances of colonial radiolaria in surface waters of the central north pacific. Journal of
511 Plankton Research 24, 797–805. <https://doi.org/10.1093/plankt/24.8.797>
- 512 Drago, L., Panaïotis, T., Irisson, J.-O., Babin, M., Biard, T., Carlotti, F., Coppola, L., Guidi, L., Hauss, H.,
513 Karp-Boss, L., Lombard, F., Mcdonnell, A.M.P., Picheral, M., Rogge, A., Waite, A.M., Stemmann, L.,
514 Kiko, R., 2022. Global Distribution of Zooplankton Biomass Estimated by In Situ Imaging and Machine
515 Learning. Frontiers in Marine Science 9. <https://doi.org/10.3389/fmars.2022.894372>
- 516 Gaskell, D.E., Ohman, M.D., Hull, P.M., 2019. Zoogliders-based measurements of planktonic foraminifera in
517 the California Current System. Journal of Foraminiferal Research 49, 390–404. <https://doi.org/10.2113/gsjfr.49.4.390>
- 518
- 519 Guidi, L., Chaffron, S., Bittner, L., Eveillard, D., Larhlimi, A., Roux, S., Darzi, Y., Audic, S., Berline,
520 L., Brum, J.R., Coelho, L.P., Espinoza, J.C.I., Malviya, S., Sunagawa, S., Dimier, C., Kandels-Lewis,
521 S., Picheral, M., Poulain, J., Searson, S., Stemmann, L., Not, F., Hingamp, P., Speich, S., Follows,
522 M., Karp-Boss, L., Boss, E., Ogata, H., Pesant, S., Weissenbach, J., Wincker, P., Acinas, S.G., Bork,

- 523 P., Vargas, C. de, Iudicone, D., Sullivan, M.B., Raes, J., Karsenti, E., Bowler, C., Gorsky, G., 2016.
- 524 Plankton networks driving carbon export in the oligotrophic ocean. *Nature* 532, 465–470. <https://doi.org/10.1038/nature16942>
- 525
- 526 Gutierrez-Rodriguez, A., Stukel, M.R., Lopes dos Santos, A., Biard, T., Scharek, R., Vaulot, D., Landry,
- 527 M.R., Not, F., 2019. High contribution of Rhizaria (Radiolaria) to vertical export in the California
- 528 Current Ecosystem revealed by DNA metabarcoding. *The ISME Journal* 13, 964–976. <https://doi.org/10.1038/s41396-018-0322-7>
- 529
- 530 Gutiérrez-Rodríguez, A., Lopes dos Santos, A., Safi, K., Probert, I., Not, F., Fernández, D., Gourvil, P.,
- 531 Bilewitch, J., Hulston, D., Pinkerton, M., Nodder, S.D., 2022. Planktonic protist diversity across con-
- 532 trasting subtropical and subantarctic waters of the southwest pacific. *Progress in Oceanography* 206,
- 533 102809. <https://doi.org/10.1016/j.pocean.2022.102809>
- 534
- 535 Haekel, E., 1887. *Report on the radiolaria collected by h.m.s. Challenger during the years 1873-1876, plates,*
- 536 Hull, P.M., Osborn, K.J., Norris, R.D., Robison, B.H., 2011. Seasonality and depth distribution of a
- 537 mesopelagic foraminifer, *Hastigerinella digitata*, in Monterey Bay, California. *Limnology and Oceanog-*
- 538 *raphy* 56, 562–576. <https://doi.org/10.4319/lo.2011.56.2.0562>
- 539 Ikenoue, T., Kimoto, K., Okazaki, Y., Sato, M., Honda, M.C., Takahashi, K., Harada, N., Fujiki, T., 2019.
- 540 Phaeodaria: An Important Carrier of Particulate Organic Carbon in the Mesopelagic Twilight Zone
- 541 of the North Pacific Ocean. *Global Biogeochemical Cycles* 33, 1146–1160. <https://doi.org/10.1029/2019GB006258>
- 542
- 543 Kimoto, K., 2015. Planktic foraminifera. pp. 129–178. https://doi.org/10.1007/978-4-431-55130-0_7
- 544 Knap, A.H., Michaels, A.F., Steinberg, D.K., Bahr, F., Bates, N.R., Bell, S., Countway, P., Close, A.R.,
- 545 Doyle, A.P., Dow, R.L., Howse, F.A., Gundersen, K., Johnson, R.J., Kelly, R., Little, R., Orcutt, K.,

- 546 Parsons, R., Rathburn, C., Sanderson, M., Stone, S., 1997. [BATS methods manual, version 4](#).
- 547 Laget, M., Drago, L., Panaïotis, T., Kiko, R., Stemmann, L., Rogge, A., Llopis-Monferrer, N., Leynaert,
548 A., Irisson, J.-O., Biard, T., 2024. Global census of the significance of giant mesopelagic protists to the
549 marine carbon and silicon cycles. *Nature Communications* 15, 3341. <https://doi.org/10.1038/s41467-024-47651-4>
- 550
- 551 Lampitt, R.S., Salter, I., Johns, D., 2009. Radiolaria: Major exporters of organic carbon to the deep ocean.
552 *Global Biogeochemical Cycles* 23. <https://doi.org/10.1029/2008GB003221>
- 553 Lee, J.J., 2006. [Algal symbiosis in larger foraminifera](#). *Symbiosis* 42, 63–75.
- 554 Llopis Monferrer, N., Biard, T., Sandin, M.M., Lombard, F., Picheral, M., Elineau, A., Guidi, L., Leynaert,
555 A., Tréguer, P.J., Not, F., 2022. [Siliceous rhizaria abundances and diversity in the mediterranean sea
556 assessed by combined imaging and metabarcoding approaches](#). *Frontiers in Marine Science* 9.
- 557 Llopis Monferrer, N., Leynaert, A., Tréguer, P., Gutiérrez-Rodríguez, A., Moriceau, B., Gallinari, M., Latasa,
558 M., L'Helguen, S., Maguer, J.-F., Safi, K., Pinkerton, M.H., Not, F., 2021. Role of small Rhizaria and
559 diatoms in the pelagic silica production of the Southern Ocean. *Limnology and Oceanography* 66, 2187–
560 2202. <https://doi.org/10.1002/lno.11743>
- 561 Lomas, M.W., Bates, N.R., Johnson, R.J., Knap, A.H., Steinberg, D.K., Carlson, C.A., 2013. Two decades
562 and counting: 24-years of sustained open ocean biogeochemical measurements in the Sargasso Sea. *Deep
563 Sea Research Part II: Topical Studies in Oceanography* 93, 16–32. <https://doi.org/10.1016/j.dsr2.2013.01.008>
- 564
- 565 Lombard, F., Boss, E., Waite, A.M., Vogt, M., Uitz, J., Stemmann, L., Sosik, H.M., Schulz, J., Romagnan,
566 J.-B., Picheral, M., Pearlman, J., Ohman, M.D., Niehoff, B., Möller, K.O., Miloslavich, P., Lara-Lpez,
567 A., Kudela, R., Lopes, R.M., Kiko, R., Karp-Boss, L., Jaffe, J.S., Iversen, M.H., Irisson, J.-O., Fennel,
568 K., Hauss, H., Guidi, L., Gorsky, G., Giering, S.L.C., Gaube, P., Gallager, S., Dubelaar, G., Cowen,

- 569 R.K., Carlotti, F., Briseño-Avena, C., Berline, L., Benoit-Bird, K., Bax, N., Batten, S., Ayata, S.D., Ar-
570 tigas, L.F., Appeltans, W., 2019. [Globally consistent quantitative observations of planktonic ecosystems](#).
571 Frontiers in Marine Science 6.
- 572 Marra, G., Wood, S.N., 2011. Practical variable selection for generalized additive models. Computational
573 Statistics & Data Analysis 55, 2372–2387. <https://doi.org/10.1016/j.csda.2011.02.004>
- 574 Mars Brisbin, M., Brunner, O.D., Grossmann, M.M., Mitarai, S., 2020. Paired high-throughput, in situ
575 imaging and high-throughput sequencing illuminate acantharian abundance and vertical distribution.
576 Limnology and Oceanography 65, 2953–2965. <https://doi.org/10.1002/lno.11567>
- 577 McGillicuddy, D.J., Robinson, A.R., Siegel, D.A., Jannasch, H.W., Johnson, R., Dickey, T.D., McNeil, J.,
578 Michaels, A.F., Knap, A.H., 1998. Influence of mesoscale eddies on new production in the Sargasso Sea.
579 Nature 394, 263–266. <https://doi.org/10.1038/28367>
- 580 Michaels, A.F., 1988. Vertical distribution and abundance of Acantharia and their symbionts. Marine
581 Biology 97, 559–569. <https://doi.org/10.1007/BF00391052>
- 582 Michaels, A.F., Caron, D.A., Swanberg, N.R., Howse, F.A., Michaels, C.M., 1995. Planktonic sarcodines
583 (Acantharia, Radiolaria, Foraminifera) in surface waters near Bermuda: abundance, biomass and vertical
584 flux. Journal of Plankton Research 17, 131–163. <https://doi.org/10.1093/plankt/17.1.131>
- 585 Michaels, A.F., Knap, A.H., 1996. Overview of the U.S. JGOFS Bermuda Atlantic Time-series Study and
586 the Hydrostation S program. Deep Sea Research Part II: Topical Studies in Oceanography 43, 157–198.
587 [https://doi.org/10.1016/0967-0645\(96\)00004-5](https://doi.org/10.1016/0967-0645(96)00004-5)
- 588 Nakamura, Y., Itagaki, H., Tuji, A., Shimode, S., Yamaguchi, A., Hidaka, K., Ogiso-Tanaka, E., 2023.
589 DNA metabarcoding focused on difficult-to-culture protists: An effective approach to clarify biological
590 interactions. Environmental Microbiology 25, 3630–3638. <https://doi.org/10.1111/1462-2920.16524>
- 591 Nakamura, Y., Suzuki, N., 2015. [Phaeodaria: Diverse marine cercozoans of world-wide distribution](#).

- 592 Springer, pp. 223–249.
- 593 Ohman, M.D., 2019. A sea of tentacles: optically discernible traits resolved from planktonic organisms in
594 situ. ICES Journal of Marine Science 76, 1959–1972. <https://doi.org/10.1093/icesjms/fsz184>
- 595 Panaïotis, T., Babin, M., Biard, T., Carlotti, F., Coppola, L., Guidi, L., Hauss, H., Karp-Boss, L., Kiko, R.,
596 Lombard, F., McDonnell, A.M.P., Picheral, M., Rogge, A., Waite, A.M., Stemmann, L., Irisson, J.-O.,
597 2023. Three major mesoplanktonic communities resolved by in situ imaging in the upper 500 m of the
598 global ocean. Global Ecology and Biogeography 32, 1991–2005. <https://doi.org/10.1111/geb.13741>
- 599 Picheral, M., Colin, S.P., Irisson, J.-O., n.d. [Ecotaxa](#).
- 600 Picheral, M., Guidi, L., Stemmann, L., Karl, D.M., Iddaoud, G., Gorsky, G., 2010. The Underwater
601 Vision Profiler 5: An advanced instrument for high spatial resolution studies of particle size spectra
602 and zooplankton. Limnology and Oceanography: Methods 8, 462–473. <https://doi.org/10.4319/lom.2010.8.462>
- 603 Sogawa, S., Nakamura, Y., Nagai, S., Nishi, N., Hidaka, K., Shimizu, Y., Setou, T., 2022. DNA metabarcoding
604 reveals vertical variation and hidden diversity of alveolata and rhizaria communities in the west-
605 ern north pacific. Deep Sea Research Part I: Oceanographic Research Papers 183, 103765. <https://doi.org/10.1016/j.dsr.2022.103765>
- 606 Stukel, M.R., Biard, T., Krause, J., Ohman, M.D., 2018. Large Phaeodaria in the twilight zone: Their role
607 in the carbon cycle. Limnology and Oceanography 63, 2579–2594. <https://doi.org/10.1002/lno.10961>
- 608 Stukel, M.R., Ohman, M.D., Kelly, T.B., Biard, T., 2019. [The roles of suspension-feeding and flux-feeding
609 zooplankton as gatekeepers of particle flux into the mesopelagic ocean in the northeast pacific](#). Frontiers
610 in Marine Science 6.
- 611 Suzuki, N., Not, F., 2015. [Biology and ecology of radiolaria](#). Springer, pp. 179–222.
- 612 Swanberg, N.R., Anderson, O.R., 1981. Collozoum caudatum sp. nov.: A giant colonial radiolarian from

- 615 equatorial and Gulf Stream waters. Deep Sea Research Part A. Oceanographic Research Papers 28,
616 1033–1047. [https://doi.org/10.1016/0198-0149\(81\)90016-9](https://doi.org/10.1016/0198-0149(81)90016-9)
- 617 Takahashi, K., Hurd, D.C., Honjo, S., 1983. Phaeodarian skeletons: Their role in silica transport to the
618 deep sea. Science 222, 616–618. <https://doi.org/10.1126/science.222.4624.616>
- 619 Whitmore, B.M., Ohman, M.D., 2021. Zooglider-measured association of zooplankton with the fine-scale
620 vertical prey field. Limnology and Oceanography 66, 3811–3827. <https://doi.org/10.1002/lno.11920>
- 621 Wood, S.N., 2017. Generalized additive models: an introduction with R, Second edition. ed, Texts in
622 statistical science. CRC Press/Taylor & Francis Group, Boca Raton London New York.
- 623 Wood, S.N., 2001. mgcv: GAMs and Generalized Ridge Regression for R 1.
- 624 Zasko, D.N., Rusanov, I.I., 2005. Vertical Distribution of Radiolarians and Their Role in Epipelagic Com-
625 munities of the East Pacific Rise and the Gulf of California. Biology Bulletin 32, 279–287. <https://doi.org/10.1007/s10525-005-0103-5>